Food Control 20 (2009) 1127–1140

Contents lists available at ScienceDirect

Food Control

journal homepage: www.elsevier.com/locate/foodcont

Dynamic optimization of the mashing process

G.A. Durand [a], M.L. Corazza [b], A.M. Blanco [a], F.C. Corazza [b,*]

[a] Planta Piloto de Ingeniería Química, PLAPIQUI (UNS-CONICET), Camino La Carrindanga, Km. 7, 8000 Bahía Blanca, Argentina
[b] Department of Food Engineering, URI – Campus de Erechim, Av. Sete de Setembro, 1621, Erechim, RS 99700-000, Brazil

ARTICLE INFO

Article history:
Received 18 July 2008
Received in revised form 26 February 2009
Accepted 15 March 2009

Keywords:
Mashing process
Dynamic optimization
Model

ABSTRACT

This work aims to demonstrate the applicability of dynamic optimization to improve the time-temperature schedule of a brewery mashing process, based on kinetic models available in the literature. The mashing process consists in the enzymatic degradation of the polysaccharides present in the malt. This is a fundamental step within the brewery activity since the composition of the mashing wort determines the quality of the final product. The main reactions that take place in the mashing are the degradation of starch, β-glucans and arabinoxylans into small chain fermentable and non-fermentable carbohydrates. The manipulation of the temperature profile of the batch reactor is the main mechanism to control the extent of the ongoing reactions. Since high temperatures favor the production of fermentable matter but also increases the concentration of undesirable species in the wort, the choice of an adequate temperature profile is not obvious. Dynamic optimization studies with a complete mashing model demonstrate that profiles of "temperature averages" of about 51 °C are preferred over typical industrial mashings of 64 °C to optimize the operation.

1. Introduction

Mashing is a key step in the beer production process. During mashing, the enzymatic degradation of the polysaccharides present in the malt takes place. Fermentable carbohydrates are produced from the degradation of the polysaccharide starch. Such carbohydrates are converted into alcohol in the fermentation step of the beer manufacturing. Non-starch polysaccharides β-glucans and arabinoxylans also degrade during mashing into smaller chain carbohydrates.

The most important reaction in the mashing process is the enzymatic hydrolysis of the gelatinized starch since it determines the produced amount of fermentable carbohydrates and therefore the alcoholic content of the final product. Therefore, a natural objective of the mashing operation is to maximize the production of such fermentable matter. However, non-fermentable carbohydrates as limit dextrins are produced in the starch hydrolysis whose concentration in the mashing product affects the organoleptic properties of the beer. Therefore it is also necessary to keep the concentration of such intermediates at adequate levels to ensure product quality.

Moreover, high concentrations of non-starch polysaccharides as β-glucans and arabinoxylans in the mashing product are known to cause processing problems in breweries such as low extract yields, poor filterability, hazes and gels formation. For this reason the minimization of such compounds in the mashing product is required to prevent negative downstream impact.

Different enzymes catalyze all the involved reactions. Since the activity of the different enzymes is highly dependent on temperature, the manipulation of such variable is the main control mechanism to reconcile the above described multiple, often conflicting, objectives of the mashing process. As the temperature rises, the reaction rates increase steeply but the enzymes are denatured faster (Hardwick, 1995; Hough, 1990). Typically, mashing is performed in a batch reactor and the imposed mashing temperature profile is a succession of increasing temperature rests designed to cover the activity temperature range of each enzyme.

Due to the importance of the brewer industry, the mashing process has been extensively studied from a modeling point of view in the last years. Kinetic models have been developed for the hydrolysis of starch and the degradation of β-glucans and arabinoxylans (Brandam, Meyer, Proth, Strehaiano, & Pingaud, 2003; Kettunen, Hamalainen, Stenholm, & Pietila, 1996; Koljonen, Hamalainen, Sjoholm, & Pietila, 1995; Li, Lu, Gu, Shi, & Mao, 2004; Marc, Engasser, Moll, & Flayeux, 1983). Moreover, studies on the effect of the different mashing parameters (temperature program, mash thickness, coarseness of grist and stirring) on the β-glucans and arabinoxylans degradation have been carried out for control purposes (Home, Pietila, & Sjoholm, 1993; Li, Yu, & Gu, 2005).

However, according to the authors' knowledge, no dynamic optimization studies with control purposes have been performed

* Corresponding author. Tel.: +55 54 3520 9000; fax: +55 54 3520 9090.
E-mail addresses: gdurand@plapiqui.edu.ar (G.A. Durand), mlcorazza@uricer.edu.br (M.L. Corazza), ablanco@plapiqui.edu.ar (A.M. Blanco), fernandac@uricer.edu.br, fernanda.corazza@pq.cnpq.br (F.C. Corazza).

0956-7135/$ - see front matter © 2009 Elsevier Ltd. All rights reserved.
doi:10.1016/j.foodcont.2009.03.004

Nomenclature

α_g	activity of α-amylase in grist (U/L)
α_g	activity of α-amylase in liquid phase (U/L)
β_g	activity of β-amylase in grist (U/L)
β	activity of β-amylase in liquid phase (U/L)
x_{starch}	concentration of starch in liquid phase (g/L)
x_{dex}	concentration of dextrins in liquid phase (g/L)
x_{gl}	concentration of glucose in liquid phase (g/L)
x_{mal}	concentration of maltose in liquid phase (g/L)
x_{mlt}	concentration of maltotriose in liquid phase (g/L)
x_{ldex}	concentration of limit dextrins in liquid phase (g/L)
A^g_{dex}	arrhenius temperature dependence function for dextrins production from starch (L/min/g)
A^g_{mlt}	arrhenius temperature dependence function for maltotriose production from starch (L/min/g)
B_{gl}	arrhenius temperature dependence function for glycose production by β-amylase (L/min/g)
B_{mal}	arrhenius temperature dependence function for maltose production by β-amylase (L/min/g)
B_{ldex}	arrhenius temperature dependence function for limit dextrins production by β-amylase (L/min/g)
k_α	arrhenius temperature dependence function for α-amylase denaturation (min^{-1})
k_β	arrhenius temperature dependence function for β-amylase denaturation (min^{-1})
b_g	activity of β-glucanase in grist (U/L)
b_w	activity of β-glucanase in liquid phase (U/L)
g_g	concentration of glucans in grist (g/L)
g_w	concentration of glucans in liquid phase (g/L)
s_g	concentration of insoluble glucans in grist (g/L)
k_w	arrhenius temperature dependence function for β-glucanase denaturation (min^{-1})
a_w	arrhenius temperature dependence function for β-glucans degradation (L/U min)
x_g	activity of endo-xylanase in grist (U/L)
x_w	activity of endo-xylanase in liquid phase (U/L)
c_g	concentration of arabinoxylans in grist (g/L)
c_w	concentration of arabinoxylans in liquid phase (g/L)
s^c_g	concentration of insoluble arabinoxylans in grist (g/L)
k^x_w	arrhenius temperature dependence function for endo-xylanase denaturation (min^{-1})
a^c_w	arrhenius temperature dependence function for arabinoxylans degradation (L/U min)

so far for the complete reaction system of the mashing process (hydrolysis of starch and degradation of β-glucans and arabinoxylans). It is the objective of this contribution to integrate in a single model the dynamics of the main mashing reactions and to perform a dynamic optimization study aimed to identify optimal temperature programs to enhance the overall mashing operation.

2. Materials and methods

In this section, the mashing model used in this work, which considers the starch, glucans and arabinoxylans degradation, is presented, together with an overview on dynamic optimization strategies and tools.

2.1. Mashing model

The schematic representation of the main reactions that take place in the mashing process is shown in Fig. 1, namely the hydrolysis of starch and the enzymatic degradation of β-glucans and arabinoxylans. In the following the kinetic model of each reaction is described and the full model presented in the Appendix section of the paper.

2.1.1. Starch hydrolysis

The adopted model for the hydrolysis of the starch is the one proposed in Koljonen et al. (1995). These authors developed the starch hydrolysis model using Finnish barley varities as Kymppi, Ingrid and Kustaa. According to this model, solid starch grains undergo a transition into a gelatinized state, which is hydrolyzed by the action of dissolved α-amylase. The hydrolysis products are maltotriose and dextrins. Dextrins are converted into sugars (glucose, maltose) and "limit dextrins" by the action of dissolved β-amylase. Limit dextrins are considered not to be further hydrolysable. The enzymes, α-amylase and β-amylase, undergo temperature deactivation. Saccharose and fructose are not included in the model since their concentration in wort is insignificant. The kinetics of the described process together with data and definitions are provided in Appendix A.

2.1.2. Glucan hydrolysis

The model used for the hydrolysis of β-glucans was developed by Kettunen et al. (1996) from the same Finnish barley varities used by Koljonen et al. (1995) in the starch hydrolysis modeling. During mashing β-glucans are extracted from the grist to the liquid phase. This process is favored by temperature. Dissolved β-glucans are converted into shorter β-oligosaccharides by the action of β-glucanases, which suffer temperature deactivation. The corresponding equations and data are presented in Appendix B.

2.1.3. Arabinoxylans degradation

The model for the degradation of arabinoxylans was taken from Li et al. (2004). These authors utilized different commercial malts in the model development: Harrington from Canada, Kendall and Schooner from Australia and KA4B from China. The arabinoxylans present in the grist dissolve and undergo a degradation into oligo-β-xylosides by the action of the endo-xylanase enzyme. Temperature favors the solubilization of the arabinoxylans as well as the denaturalization of the endo-xylanase. Equations and data are provided in Appendix C.

2.2. Overview on dynamic optimization

The problem considered in this contribution can be stated as follows (Biegler, 2007):

$$
\begin{aligned}
\min_{\mathbf{z}(t),\mathbf{u}(t),\mathbf{p}} \quad & \varphi(\mathbf{z}(t),\mathbf{u}(t),\mathbf{p}) && \text{(a)}\\
\text{s.t.} \quad & \frac{d\mathbf{z}(t)}{dt} = \mathbf{f}(\mathbf{z}(t),\mathbf{y}(t),\mathbf{u}(t),\mathbf{p}), \mathbf{z}(t_0) = \mathbf{z}_0 && \text{(b)}\\
& \mathbf{g}(\mathbf{z}(t),\mathbf{y}(t),\mathbf{u}(t),\mathbf{p}) = \mathbf{0} && \text{(c)}\\
& \mathbf{g}_f(\mathbf{z}(t)) = \mathbf{0} && \text{(d)}\\
& \mathbf{u}_L \leqslant \mathbf{u}(t) \leqslant \mathbf{u}_U &&\\
& \mathbf{y}_L \leqslant \mathbf{y}(t) \leqslant \mathbf{y}_U && \text{(e)}\\
& \mathbf{z}_L \leqslant \mathbf{z}(t) \leqslant \mathbf{z}_U &&
\end{aligned}
\tag{1}
$$

The optimization variables in problem (1) are the differential state variables $\mathbf{z}(t)$, the algebraic variables $\mathbf{y}(t)$, and the control variables, $\mathbf{u}(t)$, all functions of the scalar time parameter $t \in [t_0, t_f]$, along with

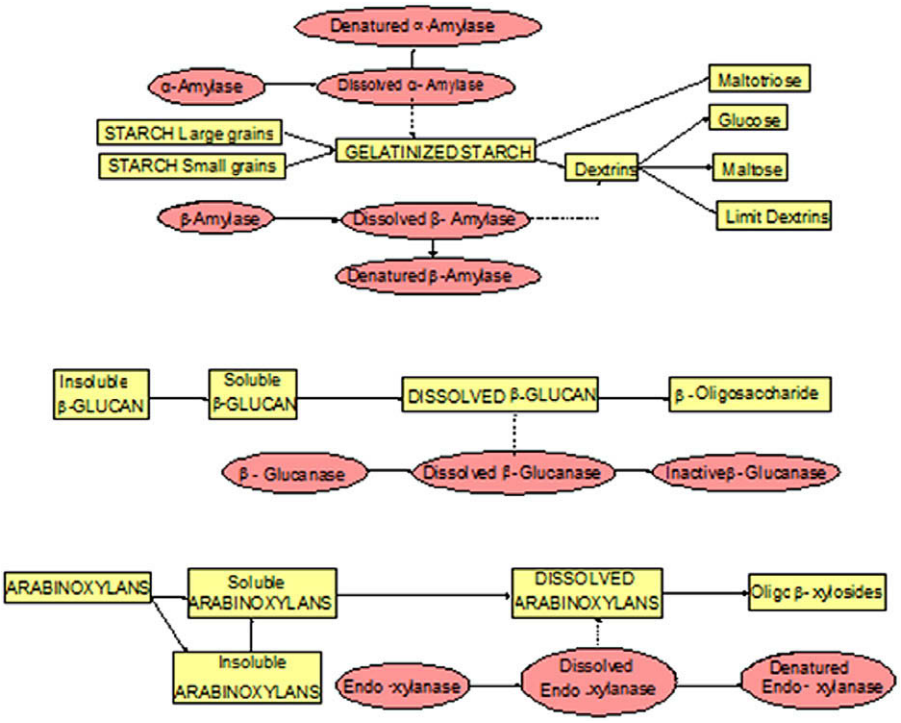

Fig. 1. Schematic representation of mashing enzymatic reactions.

the time independent parameters **p**. The objective is to optimize some performance index (1a), which is a function of the involved variables, subject to the differential algebraic system of equations (DAE) (1b–d) and to appropriate constraints on the variables (1e).

There exist a number of approaches to address problem (1), which can be broadly classified in *sequential* and *simultaneous* strategies.

In the sequential approach, also known as *control vector parameterization*, the control variables are represented as piecewise polynomials and optimization is performed with respect to the polynomial coefficients. The optimization parameters are driven by a Nonlinear Programming solver (NLP) while the DAE system is solved in each iteration within an inner loop. Sequential strategies are relatively easy to implement but the solution of the DAE system in each iteration use to be computationally expensive for large scale models.

In the simultaneous approach, also referred as *direct transcription*, both the state and the control profiles are discretized in time through collocation of finite elements. Such an approach leads to a large scale NLP problem which requires efficient solution algorithms. The simultaneous approach is usually faster than the sequential counterpart and present more flexibility in handling path inequality constraints and dealing with unstable and ill-conditioned problems. A comprehensive description of the dynamic optimization theory is beyond the scope of this contribution. The interested reader is referred for example to Biegler (2007) and references therein.

For the purposes of this study, the dynamic optimization experiments were performed with two different tools within the sequential approach.

One of the explored tools was the gProms platform (gProms User gPROMS User Guide, 2004), which provides a friendly interface to write dynamic models and linkage with efficient large scale deterministic NLP solvers. In particular, the platform makes use of a Sequential Quadratic Programming (SQP) solver and automatic differentiation routines. gProms implements a backward difference formula for the integration of the dynamic system of equations. It should be noted that the solutions obtained by gProms are local in nature since the SQP algorithm is a local NLP solver. In other words, the obtained solutions will depend on the starting point of the optimization and, therefore, will be not necessarily global.

Dynamic optimization studies were also performed using a global optimization tool, namely a stochastic NLP solver based on the Particle Swarm Optimization (PSO) strategy. The PSO is a stochastic algorithm that tries to imitate the gregarious behavior of the movement of some biological species, such as birds and fishes (Eberhart & Kennedy, 1995; Pan, Wang, & Liu, 2006). As well as the genetic algorithm, the PSO explores the space solution of the problem through the systematic evolution of a population of solutions (states) randomly generated, however the PSO presents a simpler evolutionary structure and it uses a smaller number of control parameters, what results in an efficient, robust and easy implementation algorithm. In this work, PSO algorithm was implemented in Fortran 90 language. The mashing model was integrated by fifth-order Runge–Kutta method through rkqs subroutine (Press, Teukolsky, Vetterling, & Flannery, 1992).

It should be stressed at this point that the validity of any computational study highly depends on the quality of the underlying model. The three adopted models were validated in laboratory and industrial scale mashing operations. The parameters of the kinetic equations were calculated with typical parameter identification techniques from sets of experimental data of mashings of specific industrial malts. Additionally, the models are phenomenological ones, with good extrapolation properties.

There exist alternative models other than those used in the present contribution to represent specific aspects of the mashing process (Brandam et al., 2003; Marc et al., 1983). For a specific application, the most appropriate model that describes the particular operations, as well as the specific types of malt, should be adopted. However, the applicability of dynamic optimization as a general framework to design control strategies for the mashing process remains valid.

3. Experimental

This section presents in the first place, results obtained by simulation of isothermal mashings to qualitatively assess the effect of temperature on the process. Then, the results of the dynamic optimization experiments considering the minimization of starch, limit dextrins, glucan and arabinoxylan concentrations are presented and discussed. Finally, results from additional experiments including the minimization of the batch time and with end point constraints on glucan and arabinoxylan concentrations are also presented.

3.1. Simulation studies

In order to qualitatively unravel the behavior of the different reactions taking place in the mashing process as a function of temperature, isothermal mashings of fixed duration time (115 min) were simulated for temperatures between 42 and 82 °C (315 and 355 K). For each simulation, the final concentration of each compound in the mashing product is reported in Figs. 2–5.

From Fig. 2 it can be observed that the final concentration of starch is minimal for the 67 °C (340 K) mashing, coinciding with the minimal temperature at which all the starch is gelatinized. At temperatures higher than 63 °C (336 K), starch concentration decreases linearly due to the starch gelatinization behavior also be linear, that is, it can be seen from Fig. 2 that the starch gelatinization is the limiting step until 63 °C. The largest concentration of maltotriose also occur at the 67 °C mashing although the final activity of α-amylase is significantly reduced at this temperature. In this case, maltotriose concentration is limited by the gelatinized starch concentration and not by the low α-amylase activity. At temperatures higher than 63 °C, the α-amylase activity decreases

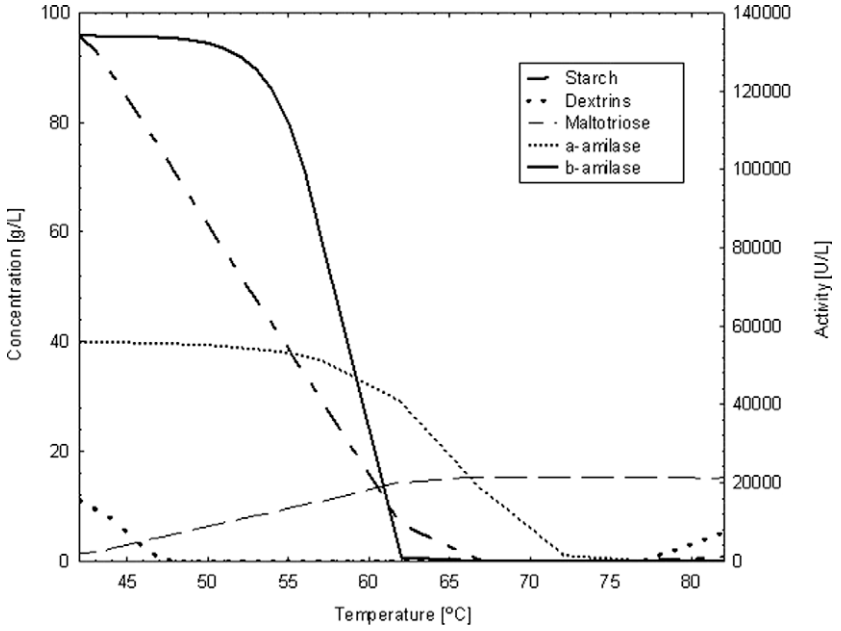

Fig. 2. Final concentrations of starch, dextrins and maltotriose and final activities of α-amylase and β-amylase for isothermal mashings.

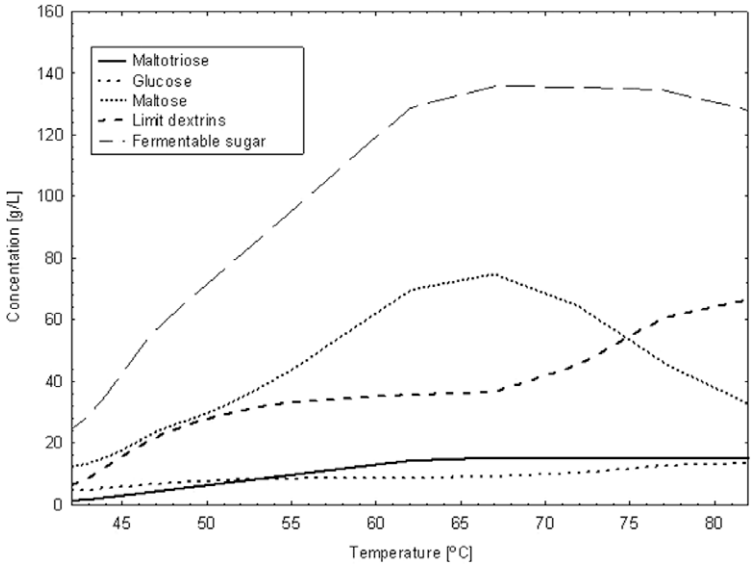

Fig. 3. Final concentrations of fermentable sugars for isothermal mashings.

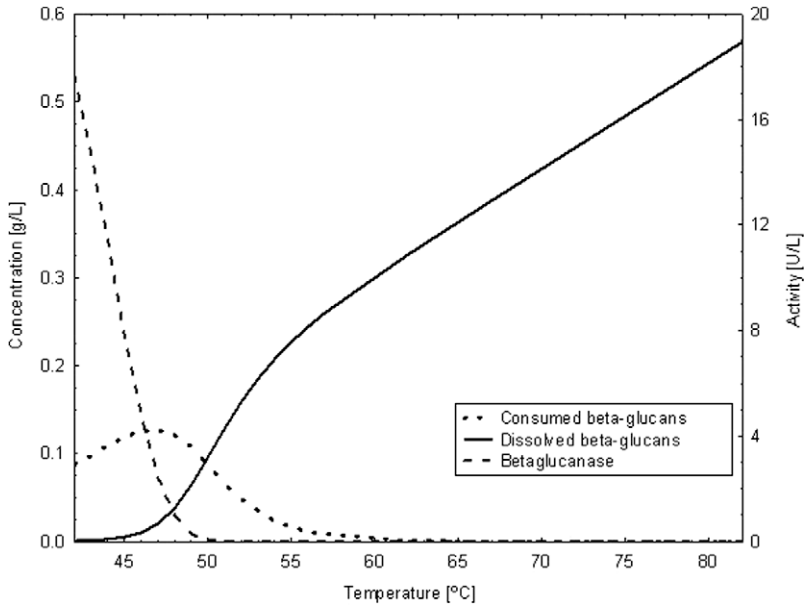

Fig. 4. Final concentrations of glucanes and final activity of β-glucanase for isothermal mashings.

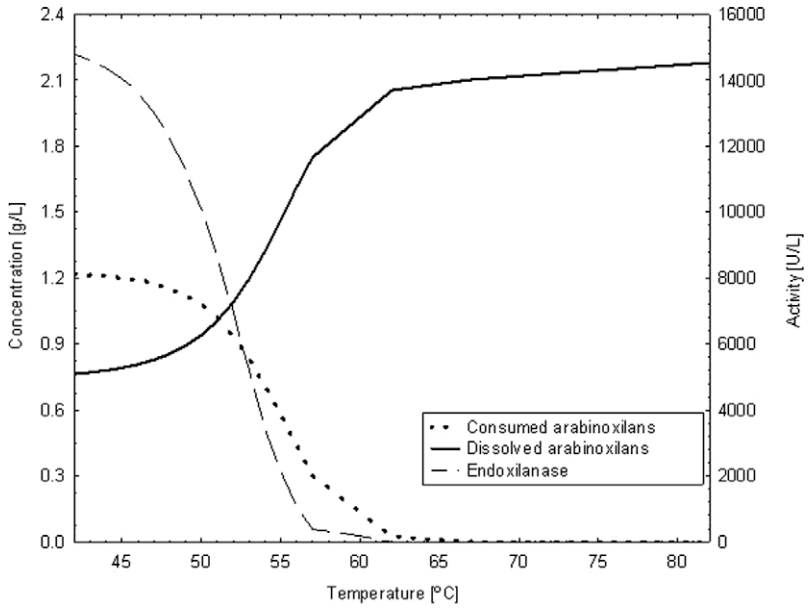

Fig. 5. Final concentrations of arabinoxylans and final activity of endo-xylanase for isothermal mashings.

but there is more available starch, supporting the maltotriose production. Dextrins undergo complete decomposition in glucose, maltose and limit dextrins at 67 °C even when the final activity of β-amylase is also small.

In Fig. 3 the final concentrations of the fermentable sugars maltotriose, glucose, maltose and limit dextrins are reported together with the summation of the individual concentrations (fermentables). It can be observed that a maximum amount of fermentable sugar is also reached in the mashing at 67 °C, confirming the relevance of the starch gelatinization step.

From the above observations it can be concluded that mashings operated at temperatures close to 67 °C favor the production of fermentable matter which is a desirable objective of the beer production process.

In Fig. 4 the behavior of β-glucans is shown for the studied isothermal mashings. The dissolution of β-glucans from the grist is favored with temperature. Low concentrations of dissolved β-glucans are observed at low temperatures (<48 °C, 321 K) when final β-glucanase activity is large and β-glucans are degraded in a large extent to β-oligosaccharides. At higher temperatures β-glucanase activity significantly decreases and quickly become inactive with the consequent increase of β-glucans concentration in the liquid phase.

A similar behavior is observed for the arabinoxylans in Fig. 5. The dissolution of arabinoxylans from the grist increases with temperature while its degradation into small oligo-β-xylosides occur at temperatures lower than 62 °C when endo-xylanase still shows significant activity.

From the above it results that in order to keep β-glucans and arabinoxylans at low concentrations in the final product it is convenient to operate the mashing at low temperatures, say less than 47 °C. This result is in conflict with the high temperatures required to optimize the hydrolysis of the starch, showing the multiple objective nature of the mashing control problem.

In the following section dynamic optimization studies are performed to investigate the effect of the temperature profile on the conflicting performance objectives of the mashing process.

3.2. Dynamic optimization studies

In order to analyze the performance of the mashing regarding the imposed temperature profile, several dynamic optimization studies have been carried out.

For comparison with current industrial practices, a typical "heuristic mashing" is considered as benchmark. Heuristic mashings are typically driven by four rests temperature profiles of similar duration (Koljonen et al., 1995). The adopted realization is detailed in Table 1 and the corresponding simulation profiles shown in Fig. 6.

In the following the major assumptions considered in the dynamic optimization studies are summarized.

In all the cases the total mashing duration was fixed in 115 min. The number of isothermal rests were also imposed. Experiences with three, four and five rests were performed. The adopted optimization variables were the temperatures and durations of each rest. Rest duration was constrained to be greater or equal than 10 min to avoid unreasonably short rests.

Table 1
Dynamic optimization results.

	T (°C)	Duration (min)
Heuristic mashing		
Rest 1	50.00	30.00
Rest 2	63.00	35.00
Rest 3	72.00	35.00
Rest 4	80.00	15.00
Average temperature (°C)	64.56	
Objective function	3.49	
Fermentable sugar concentration (g/L)	93.71	

As optimization function to be minimized it was adopted the summation of the concentration of all present polysaccharides (starch, dextrins, β-glucans and arabinoxylans). Such performance index naturally reconciles the different objectives of the mashing process: the maximization of the final concentration of fermentable sugars due to the degradation of gelatinized starch and the minimization of the final concentration of dissolved β-glucans and arabinoxylans in the mashing.

Therefore, the dynamic optimization problem for the mashing process can be stated as:

$$\begin{aligned} &\min \\ &\quad F = c_w + g_w + x_{\text{starch}} + x_{\text{dext}} \\ &\text{s.t.} \\ &\quad \frac{d\mathbf{y}}{dt} = f(t, \mathbf{y}(t), \mathbf{u}(t), \mathbf{p}), \quad \mathbf{y}(t_0) = \mathbf{y}_0 \\ &\quad \mathbf{p}_L \leqslant \mathbf{p} \leqslant \mathbf{p}_U \end{aligned} \tag{2}$$

where $\mathbf{y}$ is the state variables array and $\mathbf{p}$ is the parameter array with the rest temperatures and duration.

An average, defined as the summation of the rest temperature times the rest duration divided by the total mashing time (115 min), is also reported to provide an insight on the temperature level of each experience.

Table 2
Dynamic optimization results using gProms.

	Optimization 1		Optimization 2		Optimization 3	
	T (°C)	Duration (min)	T (°C)	Duration (min)	T (°C)	Duration (min)
Rest 1	45.02	78.18	44.32	58.64	44.79	72.95
Rest 2	59.86	16.10	50.69	23.65	56.28	11.92
Rest 3	71.37	20.72	61.33	12.71	61.42	10.00
Rest 4	–	–	71.53	19.99	71.15	13.38
Rest 5	–	–	–	–	73.38	6.74
Average temperature (°C)	51.84		52.24		52.17	
Objective function	2.01		2.00		1.96	
Fermentable sugar concentration (g/L)	95.65		94.80		94.43	
CPU time (s)[a]	8.01		10.8		9.11	

[a] Pentium 945 (1 GB ram).

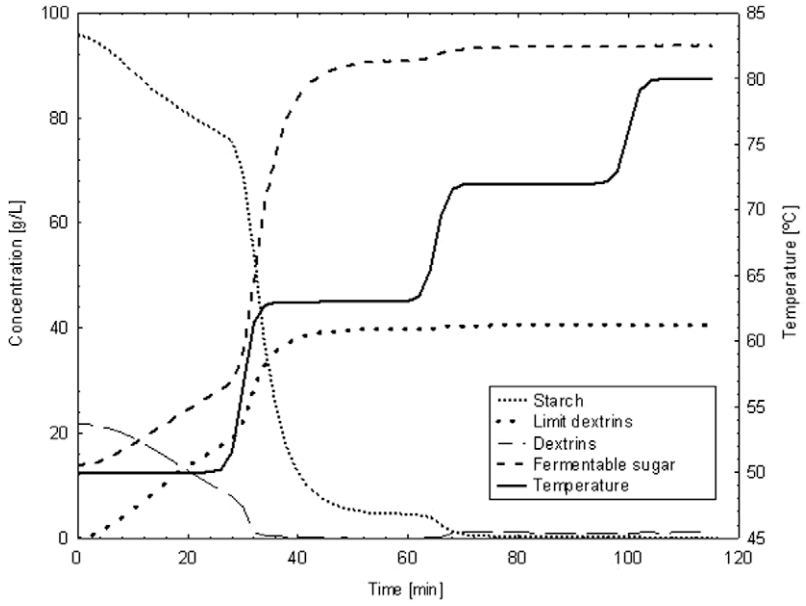

Fig. 6. Temperature and concentrations of starch, limit dextrins, dextrins and fermentable sugar profiles for the heuristic mashing.

Results for the three optimizations using gProms are summarized in Table 2 (Optimizations 1, 2 and 3). The profiles of the main variables are shown in Figs. 7–9.

From comparison of the "Heuristic" (Table 1) and "Optimized" cases using gProms (Table 2) it can be observed that the objective function significantly improves in the optimized cases. A decrease in the final polysaccharides concentration of about 42% is achieved by optimizing the temperature profile. Moreover, an increase in the concentration of fermentable sugars of about 1.3% is also observed.

This rough comparison suggests that the manipulation of the temperature profile effectively helps in the production of fermentables from starch and on the control of the non-starch polysaccharides concentration in the mashing product.

The main difference between the heuristic profile and the corresponding "four-step" optimized (Optimization 2) is the duration of the first "low temperature" rest. The first rest of the heuristic mashing covers about 26% of the whole mashing time, while for the optimized four-step mashing it lasts about 50% of the batch. In fact, an interesting feature of all the optimized profiles obtained with gProms is that the first rest is large in comparison with the others, taking between 50% and 68% of the whole mashing time.

Another difference between the heuristic and the optimized four rests profile (Table 2, Optimization 2) is that the average temperature level for each rest is lower in the optimized mashing. Moreover, all the optimized mashings are driven at a significantly lower temperature average than the heuristic mashing. This is the result of the fact that the temperature levels in the optimized cases are lower than in the heuristic case and also due to the fact that the first "low temperature rest" dominates the optimized mashings as described above.

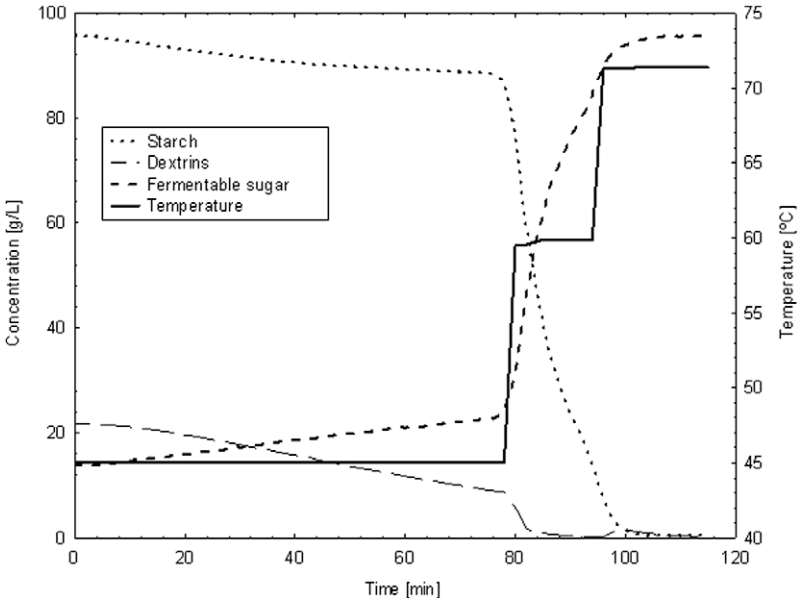

Fig. 7. Temperature and concentrations of starch, limit dextrins, dextrins and fermentable sugar profiles for the three rest mashing optimized with gProms.

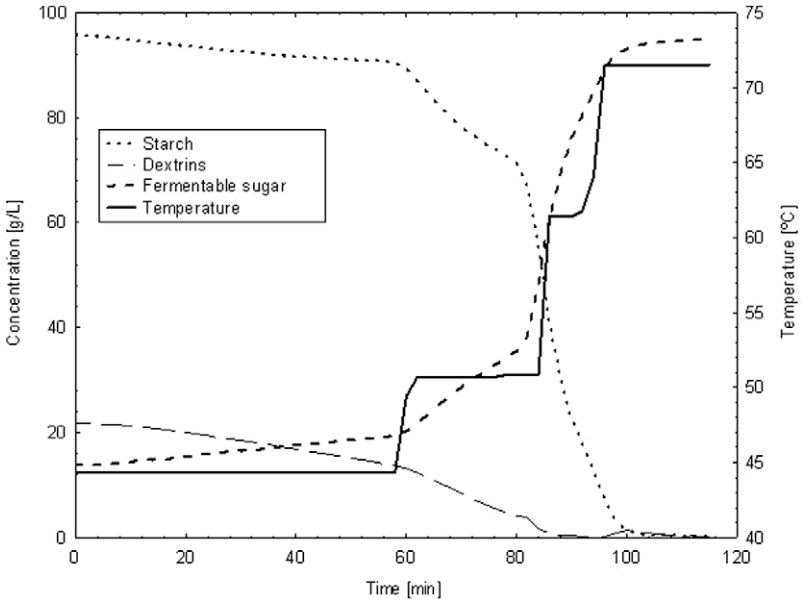

Fig. 8. Temperature and concentrations of starch, limit dextrins, dextrins and fermentable sugar profiles for the four rest mashing optimized with gProms.

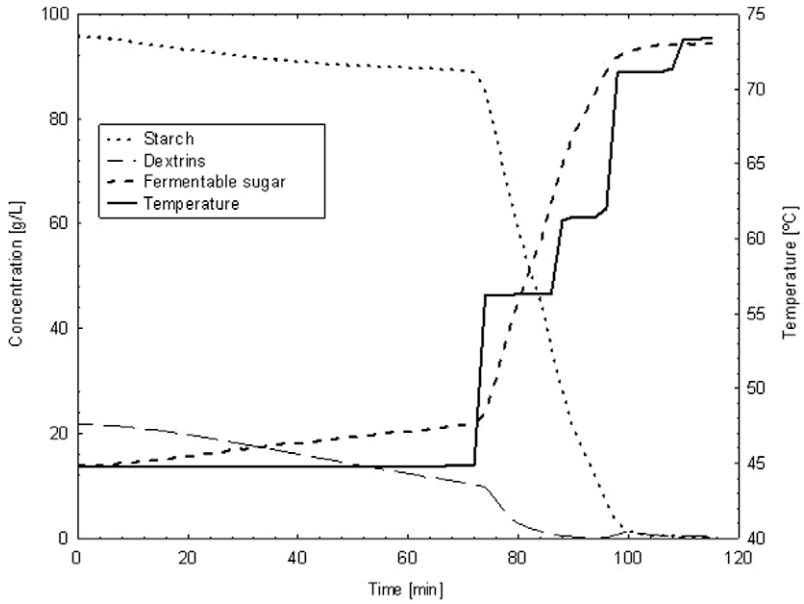

Fig. 9. Temperature and concentrations of starch, limit dextrins, dextrins and fermentable sugar profiles for the five rest mashing optimized with gProms.

Table 3
Dynamic optimization results using PSO.

	Optimization 4		Optimization 5		Optimization 6	
	T (°C)	Duration (min)	*T* (°C)	Duration (min)	*T* (°C)	Duration (min)
Rest 1	47.37	34.91	41.83	20.14	42.85	28.82
Rest 2	44.10	33.03	44.54	31.29	45.20	20.73
Rest 3	62.83	47.05	46.97	34.48	46.62	19.31
Rest 4	–	–	63.63	29.09	49.48	16.63
Rest 5	–	–	–	–	63.57	29.39
Temperature average (°C)	51.43		49.24		49.54	
Objective function	4.56		1.39		1.39	
Fermentable sugar concentration (g/L)	92.55		97.17		95.78	
CPU time (s)[a]	201.56		145.61		184.73	

[a] Pentium 4 CPU 3 GHz (488 MB ram).

From Table 2 it can be also observed that the objective function improves with the number of isothermal rests, and therefore with their level and duration. However, the differences between the absolute values of the objective function for the three studies is negligible.

Results for the three optimizations using the PSO algorithm are summarized in Table 3 (Optimizations 4, 5 and 6). The profiles of the main variables are shown in Figs. 10–12.

The results for the optimized cases with the PSO algorithm show a large improvement in both objective function and concentration of fermentable matter for the four and five rests experiments. In average (Optimizations 5 and 6) a decrease of about 60% is achieved in the total polysaccharides concentration and an increase of 2.95% in the corresponding to fermentable sugars. Again it is confirmed that the adequate manipulation of the temperature profile positively impacts the performance of the mashing process.

It can be also observed that optimized mashings 5 and 6 are driven at a significant lower average temperature than in the heuristic case. Such low temperature average is the result of the fact that while all rests have similar durations, the first rests are conducted at rather low temperatures and only the last rest shows a relatively high temperature level. In other words, there is a significant difference (18.36 °C) between the average temperature level of the first rests (45 °C) and the temperature level of the last rest (63.5 °C) in those optimized cases.

For the three rests experience however, the PSO strategy converges to a rather poor solution since better controls are known to exist (e.g. the heuristic case of Table 1 and Optimization 1 of Table 2). This result is attributed to the fact that the fitness landscape corresponding to the three rests control probably present very narrow valleys which are hard to identify with the adopted parameters for the PSO strategy. Since the tuning of the parameters of stochastic algorithms is quite problem dependant, better results are expected with an ad hoc parameterization for the three rests case. Such analysis is beyond the scope of the present study, which intends to show the general performance of state of the art dynamic optimization approaches on the mashing process.

In the following some general conclusions are summarized.

From inspection of the average temperature in all analyzed cases (Tables 1–3) it is observed that the process is carried out at an average temperature always between 48 °C and 67 °C. Such result is in agreement with the observations withdrawn from the isothermal simulations of Section 2, where it was shown that such intermediate temperatures reconcile some of the conflicting objectives of the mashing process.

It can be also noticed that, in order to optimize the performance of the mashing process, the batch should be operated at rather low "temperature averages" (close to the 48 °C bound). A representative figure for such parameter in all the optimized cases (Tables 2 and 3) is 51 °C, while the corresponding to the heuristic case is 64.41 °C.

Low temperature averages were achieved in the experiences of Table 2 with a long first low temperature rest followed by rather short high temperature rests, while in the experiences of Table 3 such low averages were achieved by similar duration low and moderate temperature rests.

The global solutions obtained using the PSO technique (Table 3) outperforms those using the local solver (Table 2) as expected. It can be concluded from those experiences that the average temperature is closer in all cases to the lower bound of 48 °C in the PSO optimizations (50 °C) than those obtained with the gProms optimizations (51.93 °C).

Regarding computation effort, it can be concluded from the CPU time reported in Tables 2 and 3 that the gProms implementation is

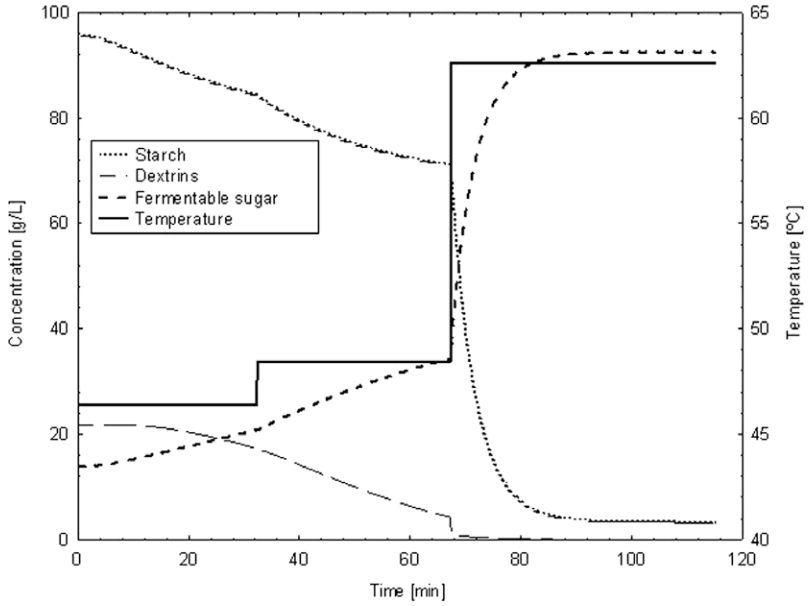

Fig. 10. Temperature and concentrations of starch, limit dextrins, dextrins and fermentable sugar profiles for the three rest mashing optimized with PSO algorithm.

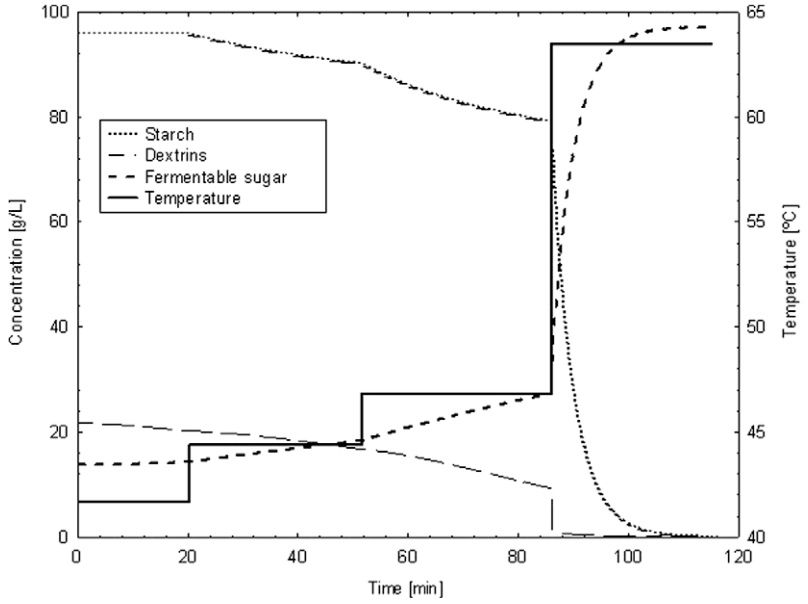

Fig. 11. Temperature and concentrations of starch, limit dextrins, dextrins and fermentable sugar profiles for the four rest mashing optimized with PSO algorithm.

more efficient than the PSO algorithm. This is a direct consequence of the use of gradient information along the search, but at the expense of a high probability of getting trapped in local optima. The PSO implementation on the other hand, present a lower performance regarding computation time due to the parallel exploration of the search space, but shows better convergence properties to global solutions as discussed above.

3.3. Additional experiments

In the previous section several experiments were presented in order to show how dynamic optimization studies could be used to improve the control of the mashing process. The adopted criterion was to minimize the final concentration of the polysaccharides present in the wort after a given batch time by applying several temperature rests of increasing values. The motivation of such an approach was to resemble typical industrial practice as reported in the literature and also to make easy a comparison between the obtained results and those previously published.

However, it should be noted that depending on the specific system, other process performance measures and quality constraints might be relevant. In fact, the selection of an objective function to evaluate process performance is to some extent subjective since most process systems are in general of "multiple objective" nature.

In this section, additional experiments are reported in order to study other possible requirements for the mashing process. Specifically, end point constraints for glucans and arabinoxilans are considered in Section 3.3.1 and the minimization of the batch time as an alternative process performance index is addressed in Section 3.3.2.

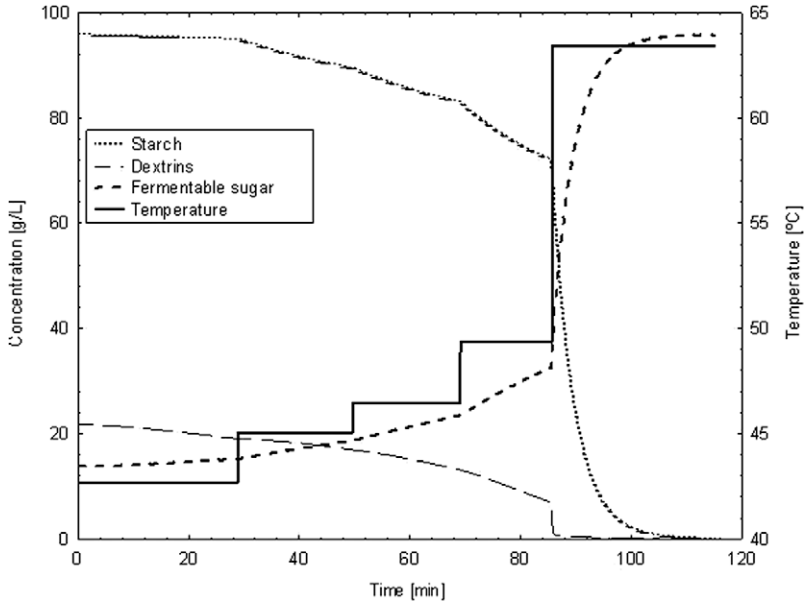

Fig. 12. Temperature and concentrations of starch, limit dextrins, dextrins and fermentable sugar profiles for the five rest mashing optimized with PSO algorithm.

3.3.1. End point constraints

The presence of β-glucans and arabinoxilans in the wort has been reported to be detrimental for downstream operations (Home et al., 1993; Sadosky & Horsley, 2002). Concerning the arabinoxilans final concentration, Li et al. (2005) pointed out the minimal possible concentration of the arabinoxilans in the wort the better for downstream process performance. However, there is still some debate on the subject since for some beers there may be a preferable "non-minimal" concentration of such compounds in the final wort provided non-occurrence of problems in lautering and filtration.

The inclusion of additional constraints is straightforward within the proposed dynamic optimization framework. If convenient levels on final concentrations of β-glucans and arabinoxilans can be identified, they can be easily included within the formulation as end point constraints in problem (2).

A series of experiences were conducted in order to minimize the final concentration of polysaccharides in the wort but imposing end point constraints on the final concentrations of the different non-starch polysaccharides. In all cases a four-step temperature profile was adopted. In the following figures the final concentration of polysaccharides and the average temperature of the mashing (first and secondary *Y-axes*, respectively) are plotted against the imposed end point constraint.

In a first set of experiences the final concentration of β-glucans was imposed in specific values and the concentration of arabinoxilans was set free to evolve without constraints. The results are shown in Fig. 13 where the objective function value is plotted as a function of the imposed end point constraint with particular values between 0.15 and 0.48 g/lt (square dot). It can be observed that the optimum objective function corresponds to an intermediate level of β-glucans concentration (about 0.26 g/lt). Smaller and larger

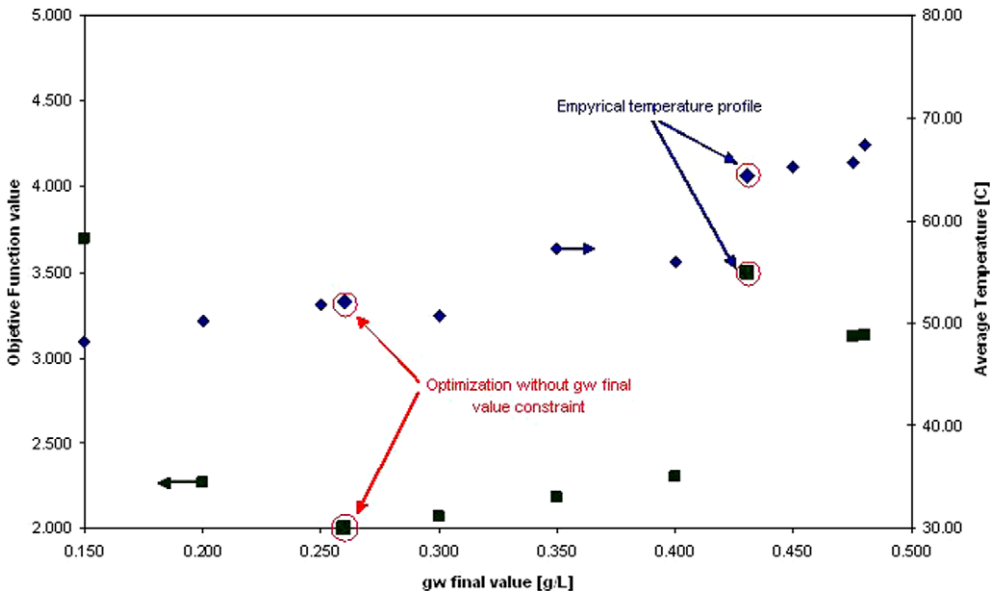

Fig. 13. Objective function value vs. final glucan concentration.

values for β-glucans final concentrations other than this intermediate level can be achieved only at the expense of increased objective function values. For comparison purposes, it is also shown in Fig. 13 the situation of the heuristic mashing which is far from the optimal operation point.

The temperature average for each experience is also indicated in Fig. 13 (diamond dot). The temperature average shows an increasing trend with the value of the end point constraint. This behavior suggests that in order to achieve large final concentrations of β-glucans in the wort, relatively high temperature rests should be favored. This is in agreement with the fact that "low average temperature mashings" are required to minimize the total polysaccharides concentration as concluded in the previous section.

A similar behavior can be appreciated from the second set of experiences where the final concentration of arabinoxilans was constrained to certain values between 0.9 and 1.4 g/lt and the corresponding to β-glucans allowed evolving without restrictions (Fig. 14). Again the optimal value of the objective function (square dots) corresponds to an intermediate level of arabinoxilans concentration (about 1.15 g/lt). As for β-glucans, other specifications than this intermediate value on the arabinoxilans can be achieved only at the expense of a worse objective function value. The temperature average of the mashing profiles (diamond dots) also shows a similar trend than in the pervious case. In order to achieve larger concentrations of arabinoxilans in the wort higher temperature average profiles should be adopted.

Finally, a third set of experiences was conducted imposing an end point constraint on the sum of the final concentrations of β-glucans and arabinoxilans. The results for a range between 1.1 and 2.4 g/lt are shown in Fig. 15. As in the previous experiences, the optimal value corresponds to an intermediate figure (about

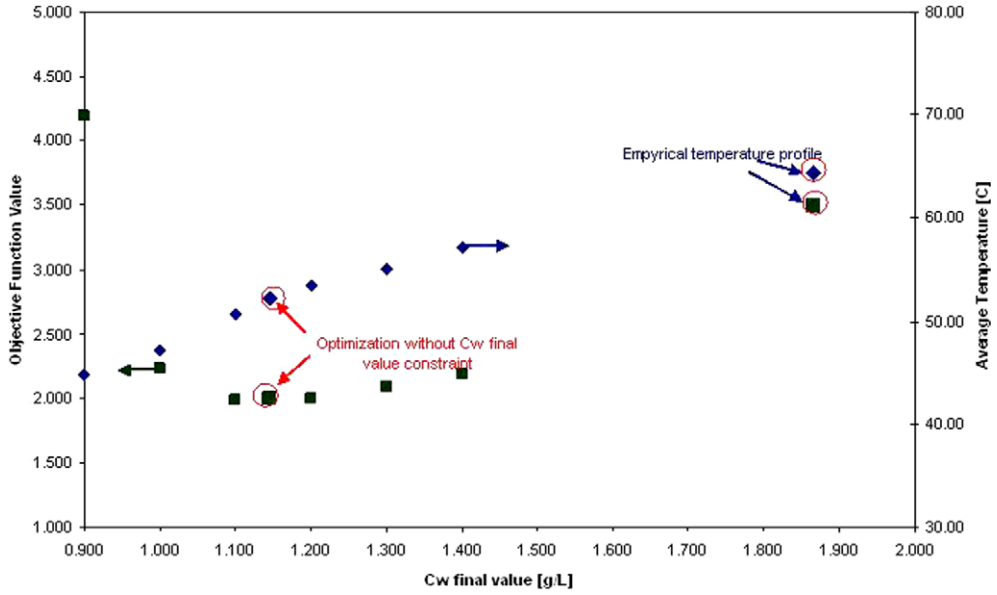

Fig. 14. Objective function value vs. final arabinoxilans concentration.

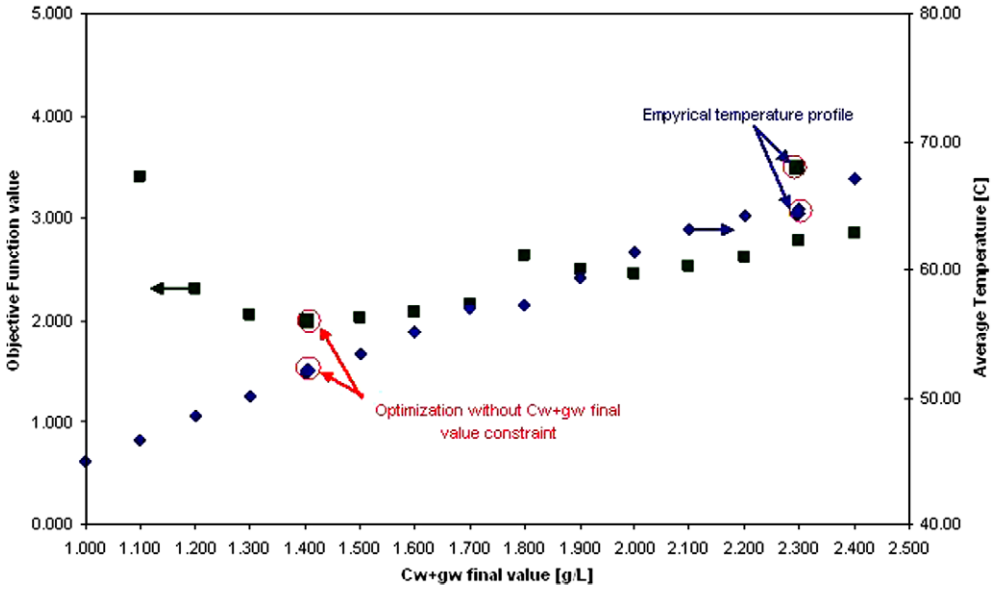

Fig. 15. Objective function value vs. final glucans + arabinoxilans concentration.

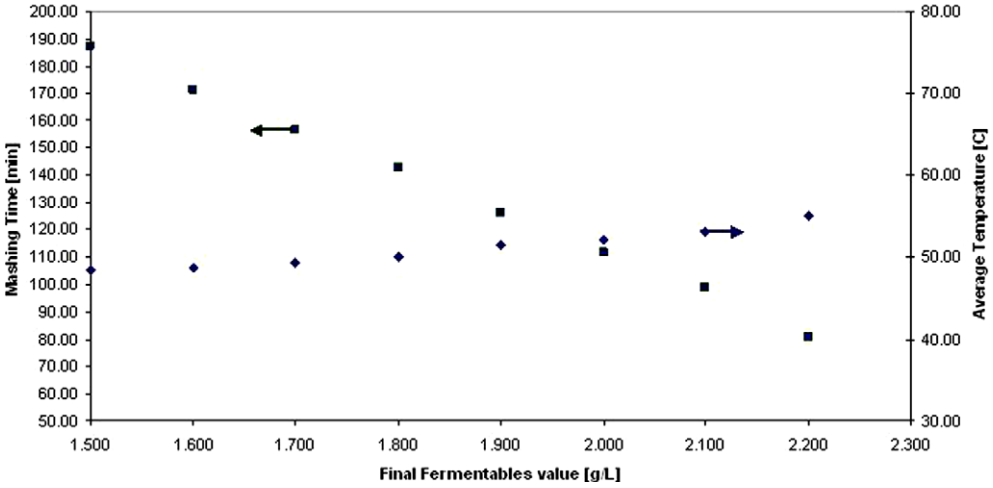

Fig. 16. Batch time vs. final concentration of fermentable material.

1.4 g/lt). Other end point concentration values than this optimal level are detrimental for the adopted objective function. There is also a clear correlation between the mashing temperature average and the imposed end point constraint: as in the previous cases, larger concentrations of the sum of β-glucans and arabinoxilans require higher average temperate profiles.

The behavior observed clearly shows the multiple objective nature of the problem under study where one objective can be improved only at the expense of the others.

3.3.2. Minimization of the batch time

While the final concentration of the fermentable polysaccharides is indeed a sound objective for the mashing process, another typical performance index for batch processes is the batch time to be minimized. In order to demonstrate the tradeoff between both objectives, additional experiments were conducted by minimizing the batch time for specific final concentrations of fermentable material in the wort. A four-step temperature profile was adopted in all cases.

The results are reported in Fig. 16 where the optimum mashing time is plotted against the imposed final concentration of fermentable polysaccharides (square dot). The corresponding average temperature is also plotted as a secondary *Y-axe* (diamond dot).

As expected, the lower the final concentration of fermentable material imposed, the larger the minimum batch time required to accomplish the constraint. The relation presents a rather linear trend in the studied range (1.2–2.3 g/lt). Regarding the temperature profile, in accordance with the results presented in Section 3.2, low average temperature profiles favor low final concentration of fermentable polysaccharides in the wort.

In this case, it can be also observed the typical behavior of multiple objective systems where one objective can be improved only at the expense of the others.

4. Conclusions and future work

In this contribution the mashing process was addressed from a dynamic optimization approach. Since high temperatures favor starch decomposition (and therefore fermentable sugars production) but also contribute to the concentration in wort of β-glucans and arabinoxylans (which degrades the quality of the mashing product), the selection of an adequate temperature profile to drive the batch is not obvious.

Global and local algorithms were used to minimize the objective function. Results obtained with both algorithms showed an improvement in the objective function and in the concentration of fermentable sugars; however, the global algorithm presented a better performance compared to the local one for the four and five rest mashings.

For comparison purposes, a "temperature average" was defined as the summation of the temperature times the duration of each rest divided by the total mashing time. A major conclusion from the dynamic optimization experiences conducted in this study is that, in order to minimize the overall concentration of polysaccharides (a significant objective function), "low temperature average" profiles of about 51 °C should be preferred over typical industrial "heuristic" profiles of about 64° C to run the mashing process.

In order to extend the scope of the dynamic optimization approach, additional studies by imposing end point constraints on β-glucans and arabinoxylans concentrations were conducted. Such studies showed that in order to achieve a specific level on a certain concentration, the overall objective necessarily worsens with respect the unconstrained case.

Finally, an additional set of experiences, which considered an alternative performance index, namely the minimization of the batch time, was carried out. A clear tradeoff between this objective function and the previously adopted was observed, which demonstrates the multiple objective nature of the mashing process.

As future work additional control strategies might be explored. For example, the adoption of heat stable enzymes can contribute to perform tighter control of the operation. It has been reported (Kettunen et al., 1996) that heat stable β-glucanase is currently used in breweries to avoid problems caused by β-glucans. A systematic dynamic optimization study, which includes heat stable enzymes might motivate future contribution on the subject.

Acknowledgements

This work was partially supported by "Concejo Nacional de Investigaciones Científicas y Técnicas" and "Universidad Nacional del Sur" of Argentina, and CNPq of Brazil.

Appendix A. Starch hydrolysis (Koljonen et al., 1995)

$$\frac{d\alpha_g}{dt} = -H_\alpha \frac{M}{V_g}(\alpha_g - \alpha) \tag{3}$$

$$\frac{d\alpha}{dt} = H_\alpha \frac{M}{V_g}(\alpha_g - \alpha) - k_\alpha \alpha \tag{4}$$

$$\frac{d\beta_g}{dt} = -H_\beta \frac{M}{V}(\beta_g - \beta) \tag{5}$$

$$\frac{d\beta}{dt} = H_\beta \frac{M}{V}(\beta_g - \beta) - k_\beta \beta \tag{6}$$

$$\frac{dx_{\text{starch}}}{dt} = -\alpha(x_{\text{starch}} - u)(0.964A^g_{\text{mlt}} + A^g_{\text{dex}}) \tag{7}$$

$$\frac{dx_{\text{dex}}}{dt} = \alpha(x_{\text{starch}} - u)A^g_{\text{dex}} - \beta x_{\text{dex}}\left(0.9B_{\text{gl}} + 0.947\frac{B_{\text{mal}}}{K_m + x_{\text{dex}}} + B_{\text{ldex}}\right) \tag{8}$$

$$\frac{dx_{\text{gl}}}{dt} = B_{\text{gl}}\beta x_{\text{dex}} \tag{9}$$

$$\frac{dx_{\text{mal}}}{dt} = \frac{B_{\text{mal}}\beta x_{\text{dex}}}{K_m + x_{\text{dex}}} \tag{10}$$

$$\frac{dx_{\text{mlt}}}{dt} = A^g_{\text{mlt}}\alpha(x_{\text{starch}} - u) \tag{11}$$

$$\frac{dx_{\text{ldex}}}{dt} = B_{\text{ldex}}\beta x_{\text{ldex}} \tag{12}$$

$$u = \begin{cases} x_{\text{starch}}(0) & T < T_u \\ \left(\frac{T}{T_u - T_g} + \frac{T}{T_g - T_u}\right) & T_u \le T \le T_g \\ 0 & T > T_g \end{cases} \tag{13}$$

$$A^g_{\text{dex}} = A^{0,g}_{\text{dex}} \exp\left(\frac{E^\alpha}{RT}\right) \tag{14}$$

$$A^g_{\text{mlt}} = A^{0,g}_{\text{mlt}} \exp\left(\frac{E^\alpha}{RT}\right) \tag{15}$$

$$B_{\text{gl}} = B^0_{\text{gl}} \exp\left(\frac{E^\beta}{RT}\right) \tag{16}$$

$$B_{\text{mal}} = B^0_{\text{mal}} \exp\left(\frac{E^\beta}{RT}\right) \tag{17}$$

$$B_{\text{ldex}} = B^0_{\text{ldex}} \exp\left(\frac{E^\beta}{RT}\right) \tag{18}$$

$$k_\alpha = k^0_\alpha \exp\left(\frac{E^\alpha_d}{RT}\right) \tag{19}$$

$$k_\beta = k^0_\beta \exp\left(\frac{E^\beta_d}{RT}\right) \tag{20}$$

Table A1
Model parameters for starch hydrolysis.

H_α	Dissolution coefficient of α-amylase	9.72E5	L/g/min
H_β	Dissolution coefficient of β-amylase	7.57E5	L/g/min
A^{0g}_{dex}	Pre-exponential factor	3.77E10	L/min/g
A^{0g}_{mlt}	Pre-exponential factor	6.42E9	L/min/g
B^0_{gl}	Pre-exponential factor	1.62E40	L/min/g
B^0_{mal}	Pre-exponential factor	1.05E42	L/min^2/g
B^0_{ldex}	Pre-exponential coefficient	1.09E41	L/min/g
k^0_α	Pre-exponential coefficient	3.86E34	min^{-1}
k^0_β	Pre-exponential coefficient	9.46E67	min^{-1}
E^α	Activation energy	1.03E5	J/mol
E^β	Activation energy	2.93E5	J/mol
E^α_d	Activation energy	2.377E5	J/mol
E^β_d	Activation energy	4.439E5	J/mol
T_u	Un-gelatinezed temperature	315.4	K
T_g	Gelatinezed temperature	336.5	K
K_m	Michelis Menten constant	2.8	g/L

Table A2
Simulation data for starch hydrolysis.

V	Volume of liquid phase	30	m^3
V_g	Volume of wet malt	4395.2	m^3
M	Initial weight of malt	6700	kg
x^0_{starch}	Initial concentration of starch in liquid phase	95.7	g/L
x^0_{dex}	Initial concentration of dextrins in liquid phase	21.7	g/L
x^0_{gl}	Initial concentration of glucose in liquid phase	3.6	g/L
x^0_{mal}	Initial concentration of maltose in liquid phase	8.9	g/L
x^0_{mlt}	Initial concentration of maltotriose in liquid phase	1.3	g/L
x^0_{ldex}	Initial concentration of limit dextrins in liquid phase	0	g/L
α^0	Initial activity of α-amylase	4.37E5	U/L
β^0	Initial activity of β-amylase	1.05E6	U/L

Appendix B. Glucan hydrolysis (Kettunen et al., 1996)

$$\frac{db_g}{dt} = -H_b \frac{M}{V_g}(b_g - b_w) \tag{21}$$

$$\frac{db_w}{dt} = -H_b \frac{M}{V_w}(b_g - b_w) - k_w b_w \tag{22}$$

$$k_w = K_{w0} \exp\left(\frac{E^k_w}{RT}\right) \tag{23}$$

$$\frac{dg_g}{dt} = -H_g \frac{M}{V_g}(g_g - s_g) \tag{24}$$

$$\frac{dg_w}{dt} = H_g \frac{M}{V_w}(g_g - s_g) - a_w b_w g_w \tag{25}$$

$$s_g = -S_g T + S_{g0} \tag{26}$$

$$a_w = A_{w0} \tag{27}$$

Table B1
Model parameters for glucan hydrolysis.

H_b	Dissolution coefficient of β-glucanase	2.28 E4	U/L
K_{w0}	Pre-exponential factor	5.30 E43	min^{-1}
E^k_w	Activation energy	277,700	J/mol
H_g	Dissolution coefficients of β-glucanes	3.56 E5	L/g/min
A_{w0}	Pre-exponential factor	2.71 E3	L/U/min
S_g	Parameter of insoluble β-glucanes concentration function	8.21 E2	g/L/K
S_{g0}	Parameter of insoluble β-glucanes concentration function	32.3	g/L

Table B2
Simulation data for glucan hydrolysis.

$b_g(0)$	Initial activity of β-glucanase in grist	220	U/L
$b_w(0)$	Initial activity of β-glucanase in liquid phase	0	U/L
$g_g(0)$	Initial activity of β-glucanes in grist	7.04	g/L
$g_w(0)$	Initial activity of β-glucanes in liquid phase	0	g/L

Table C1
Model parameters for arabinoxylans degradation.

H_x	Dissolution coefficient of endo-xylanase	2.01 E2	L/g/min
K^x_{w0}	Pre-exponential factor	2.98 E42	min^{-1}
E^x_w	Activation energy	277,400	J/mol
H_c	Dissolution coefficients of arabinoxylans	1.21 E5	L/g/min
A^c_{w0}	Pre-exponential factor	9.12 E7	L/U/min
S^c_g	Parameter of insoluble arabinoxylans concentration function	3.86 E2	g/L/K
S^c_{g0}	Parameter of insoluble arabinoxylans concentration function	65.2	g/L

Table C2
Simulation data for arabinoxylans degradation.

$x_g(0)$	Initial activity of endo-xylanase in grist	119,240	U/L
$x_w(0)$	Initial activity of endo-xylanase in liquid phase	0	U/L
$c_g(0)$	Initial activity of arabinoxylans in grist	68.4	g/L
$c_w(0)$	Initial activity of arabinoxylans in liquid phase	0	g/L

Appendix C. Arabinoxylans degradation (Li et al., 2004)

$$\frac{dx_g}{dt} = -H_x \frac{M}{V_g}(x_g - x_w) \tag{28}$$

$$\frac{dx_w}{dt} = H_x \frac{M}{V_w}(x_g - x_w) - k_w^x x_w \tag{29}$$

$$k_w^x = K_{w0}^x \exp\left(\frac{E_w^x}{RT}\right) \tag{30}$$

$$\frac{dc_g}{dt} = -H_c \frac{M}{V_g}(c_g - s_g^c) \tag{31}$$

$$\frac{dc_w}{dt} = H_c \frac{M}{V_w}(g_g - s_g^c) - a_w^c x_w c_w \tag{32}$$

$$s_g^c = -S_g^c T + S_{g0}^c \tag{33}$$

$$a_w^c = A_{w0}^c \tag{34}$$

See Tables A1, A2, B1, B2, C1, C2.

References

Biegler, L. T. (2007). An overview of simultaneous strategies for dynamic optimization. *Chemical Engineering and Processing, 46*, 1043–1053.

Brandam, C., Meyer, X. M., Proth, J., Strehaiano, P., & Pingaud, H. (2003). An original kinetic model for the enzymatic hydrolysis of starch during mashing. *Biochemical Engineering Journal, 13*, 43–52.

Eberhart, R., & Kennedy, J. (1995). New optimizer using particle swarm theory. In *Proceedings of international symposium on micro machine and human science*. Nagoya, Japan.

gPROMS Advanced User Guide (2004). Process Systems Enterprise Ltd.

Hardwick, W. A. (1995). *Handbook of brewing*. New York: Marcel Dekker Inc..

Home, S., Pietila, K., & Sjoholm, K. (1993). Control of glucanolysis in mashing. *ASBC Journal, 51*(3), 108–113.

Hough, J. S. (1990). *Biotecnología de la cerveza y de la malta*. Ed. Acribia, Zaragoza, Spain.

Kettunen, A., Hamalainen, J. J., Stenholm, K., & Pietila, K. (1996). A model for the prediction of β-Glucanase activity and β-glucan concentration during mashing. *Journal of Food Engineering, 29*, 185–200.

Koljonen, T., Hamalainen, J. J., Sjoholm, K., & Pietila, K. (1995). A model for the prediction of fermentable sugar concentrations during mashing. *Journal of Food Engineering, 26*, 329–350.

Li, Y., Lu, J., Gu, G., Shi, Z., & Mao, Z. (2004). Mathematical modeling for prediction of endo-xylanase activity and arabinolylans concentration during mashing of barley malts for brewing. *Biotechnology Letters, 26*, 779–785.

Li, Y., Yu, J., & Gu, G. (2005). Control of arabinoxylan solubilization and hydrolysis in mashing. *Food Chemistry, 90*, 101–108.

Marc, A., Engasser, J. M., Moll, M., & Flayeux, R. (1983). A kinetic model of starch hydrolysis by α- and β-amylase during mashing. *Biotechnology and Bioengineering, 28*, 481–496.

Pan, H., Wang, L., & Liu, B. (2006). Particle swarm optimization for function optimization in noisy environment. *Applied Mathematics and Computation, 181*, 908–919.

Press, W. H., Teukolsky, S. A., Vetterling, W. T., & Flannery, B. P. (1992). *Numerical recipes in FORTRAN* (2nd ed.). USA: Cambridge University Press.

Sadosky, P., Swarz, P., & Horsley, R. D. (2002). Effect of Arabinolylans, β-glucans and Dextrins on the viscosity and membrane filterability of a beer model solution. *ASBC Journal, 60*(1), 153–161.